National Conference with International Participation

ENGINEERING MECHANICS 2008

Svratka, Czech Republic, May 12 – 15, 2008

THE DEVICE FOR IMPLANTS TESTING: THE DESIGN OF CONTROL

T. Březina [*], L. Březina [**]

Summary: *The contribution presents one of control design possibilities for the cord implants testing device which is realized as Stewart platform. The controllers have relatively simple linear structure and allow to tune eigenvalues of the controlling device. Sufficient positioning accuracy and satisfactory robustness of the designed control was verified by numerous simulations.*

1. Introduction

The device for cord implants testing was designed in such a way that its movements are as close as possible to the real physiological movements. General motion and effector action forces are simulated by parallel mechanism called Stewart platform (hexapod). Typically the hexapod structure has six linearly actuated legs, these are connected to the base plate and the top (mobile) plate by universal joints located at both ends of the each leg. The six DOF top plate position and orientation depend on the length of each leg. Hexapod control task is mostly defined as tracking task of prescribed trajectories of position and orientation of its top plate masspoint. The control of hexapod is not a simple task in general, it depends on requests placed to speed and control quality, etc.

With respect to large variance of specimen parameters (spinal elements), which should be tested by hexapod, it is not necessary by definition to require high precision of control and with respect to periods of typical loading cycles of human body segments it is not also necessary to request high speed of control. That is why the conception was designed which leads onto the use of simple linear control laws.

2. The control concept

The two layer control structure was designed for the hexapod control. The higher layer solves the position control $\mathbf{m} \rightarrow \mathbf{q}$, where $\mathbf{m} = \left(M_1, \mathbf{K}, M_6\right)^T$ is the column vector of actuating

[*] doc. RNDr. Ing Tomáš Březina: Institute of Automation and Computer Science, Faculty of Mechanical Engineering, Brno University of Technology; Technická 2, 616 69, Brno; Tel. +420 541 142 295; e-mail: brezina@fme.vutbr.cz

[**] Ing Lukáš Březina: Institute of Solid Mechanics, Mechatronics and Biomechanics, Faculty of Mechanical Engineering, Brno University of Technology; Technická 2, 616 69, Brno; Tel. +420 541 143 375; e-mail: ybrezi00@stud.fme.vutbr.cz

torques for the each leg and $\mathbf{q} = (j_1, \mathbf{K}, j_6)$ is the vector of corresponding ball screw angular displacements. The layer's purpose is to synchronize actuators to reach the desired top plate motion. The vectors of corresponding ball screw angular displacements needed to reach the desired motion are generated by a trajectory generator from prescribed (reference) position and orientation of top plate masspoint. The structure of layer can be seen in Fig. 1.

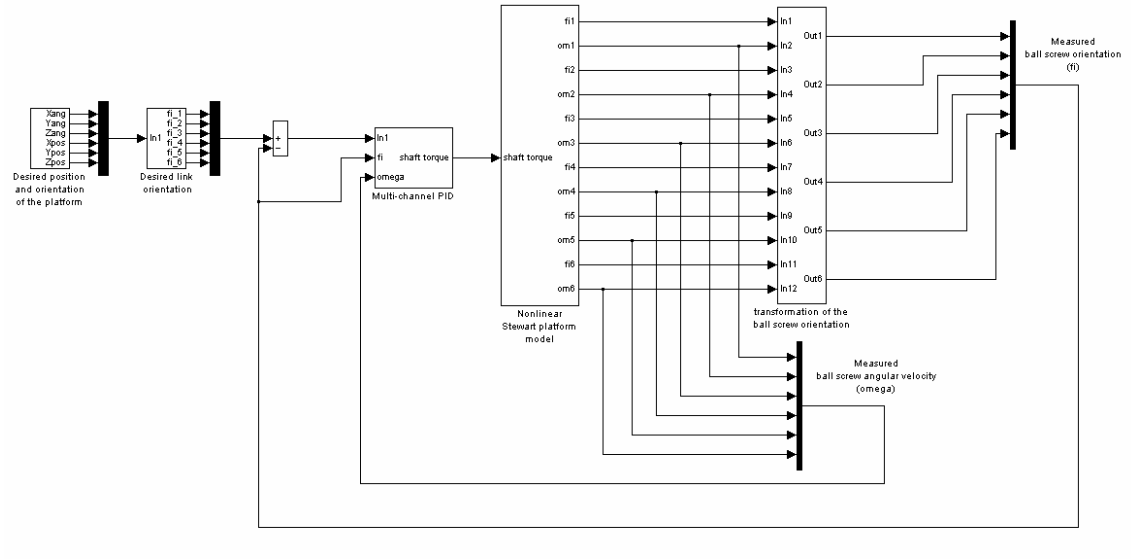

Fig. 1: Structure of higher control layer

The lower control layer contains isolated torque control of the each linear actuator $u_i \to M_i$, $i = 1, \mathbf{K}, 6$, where u_i is an input voltage of the i–th actuator and M_i is the shaft torque (Fig. 2).

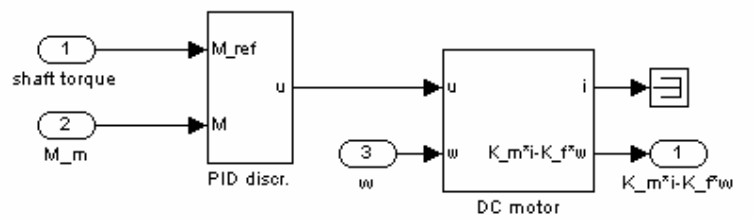

Fig. 2: Open loop of lower control layer

2.1. The design of the controllers for the lower control layer

DC motor state-space outer description was used for the control design

$$LJ\ddot{M}_m + (LK_f + RJ)\dot{M}_m + (RK_f + K_bK_m)M_m = K_mJ\ddot{\alpha} - K_fL\dot{M}_z - (RK_f + K_bK_m)M_z, \quad (1)$$

where K_m, K_b are the torque and the voltage constant, J is the moment of inertia, K_f is a linear approximation for viscous friction, M_z, M_m is a load torque and a shaft torque and finally R is the resistance and L the inductance of the armature. The model parameters were

obtained from the measured data through NI LabView System Identification Toolkit. The control law for the dynamics compensation was shaped in the form

$$u = \int_0^t \left(k_i \int_0^t \left((M_m)_{ref} - M_m \right) du - k_p M_m - k_d \dot{M}_m \right) dt \ . \tag{2}$$

Its use with choice of $k_d = \left(3pLJ - LK_f - RJ\right) \big/ \left(K_m J\right)$, $k_p = \left(3p^2 LJ - RK_f - K_b K_m\right) \big/ \left(K_m J\right)$, $k_i = \left(p^3 L\right) \big/ K_m$, leads for $p > 0$ to stable dynamics on aperiodicity margin (keeping $M_z = \dot{M}_z = 0$) by

$$\ddot{\ddot{M}}_m + 3p\ddot{\dot{M}}_m + 3p^2 \dot{M}_m + p^3 M_m = p^3 \left(M_m\right)_{ref} \tag{3}$$

and in steady state it is true that $M_m = \left(M_m\right)_{ref}$.

2.2. The design of the controller for the higher control layer

The higher layer controller has to provide robust behaviour of the whole system, numerical accuracy and easy implementation. The controller also has to eliminate actuators interaction. The linear model, numerically extracted from the model of hexapod dynamics in Matlab-SimMechanics, was used for design as

$$\ddot{\mathbf{q}} = \mathbf{C}\mathbf{q} + \mathbf{B}\dot{\mathbf{q}} + \mathbf{D}\mathbf{m} \,, \tag{4}$$

where $\mathbf{C}$ is the matrix of stiffness, $\mathbf{B}$ the matrix of damping and $\mathbf{D}$ the transformational matrix of input torques. All matrices are of type $6/6$.

The control law (multichannel PID) was used for the dynamics compensation, this time as

$$\mathbf{m} = \mathbf{K}_i \int_0^t \left(\mathbf{q}_{ref} - \mathbf{q} \right) dt \ - \mathbf{K}_p \mathbf{q} - \mathbf{K}_d \dot{\mathbf{q}} \,. \tag{5}$$

When choosing $\mathbf{K}_p = \mathbf{D}^{-1}\left(3p^2\mathbf{I} + \mathbf{C}\right)$, $\mathbf{K}_d = \mathbf{D}^{-1}\left(3p\mathbf{I} + \mathbf{B}\right)$, $\mathbf{K}_i = p^3\mathbf{D}^{-1}$ ($\mathbf{D}$ is regular) the compensated hexapod dynamics is, for $p > 0$, stable on aperiodicity margin according to

$$\dddot{\mathbf{q}} + 3p\ddot{\mathbf{q}} + 3p^2\dot{\mathbf{q}} + p^3\mathbf{q} = p^3\mathbf{q}_{ref} \,. \tag{6}$$

and it is valid in steady state that $\mathbf{q} = \mathbf{q}_{ref}$. In addition no leg behaviour depends on behaviour of other legs.

3. Notes to discretization

The continuous control laws were approximated by discrete laws and an appropriate sampling period, T_s, of discrete law was found, for the purpose of numeric control realization.

3.1. Lower control layer discretization

S–image of lower control layer law (Eq. 2) is, with zero initial conditions,

$$u(s)=\frac{1}{s}\frac{k_i\left(M_m\right)_{ref}(s)}{s}-\frac{1}{s}\left(\frac{k_iM_m(s)}{s}+k_pM_m(s)+sk_dM_m(s)\right). \tag{7}$$

A changeover to discrete domain (to z–image of transfer function) by substitutions

$$s\approx\frac{z-1}{T_sz},\ \frac{1}{s}\approx\frac{T_s}{z-1} \tag{8}$$

was proven by simulations as practically insufficient. Lower controlling subsystem is unstable even with the sampling period $T_s=10\ ms$ – moment of controlled motor continuously oscillates.

Application of s–image control law shaped as

$$u(s)=\frac{k_i\left(M_m\right)_{ref}(s)}{s^2}-\frac{s^2k_d+sk_p+k_d}{s^2}M_m(s) \tag{9}$$

and its discrete approximation obtained numerically by bilinear Tustin transformation in the form

$$u(z)=\frac{a_1z+a_0}{(z-1)^2}\left(M_m\right)_{ref}(z)-\frac{z^2b_2-b_1z-b_0}{(z-1)^2}M_m(z), \tag{10}$$

$a_0,a_1,b_2,b_1,b_0>0$, is already practicable (for controller structure see Fig. 3). The control system is stable in this case starting with $T_s\approx100\ ms$.

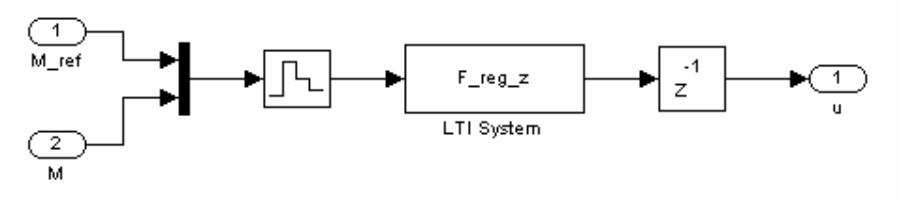

Fig. 3: Controller structure for lower layer control law

3.2. Higher control layer discretization

In the case of control law of multichannel PID (Eq. 5) with s–image of control law for zero initial conditions

$$\mathbf{m}(s)=\frac{\mathbf{K}_i}{s}\left(\mathbf{q}_{ref}(s)-\mathbf{q}(s)\right)-\mathbf{K}_p\mathbf{q}(s)-s\mathbf{K}_d\mathbf{q}(s). \tag{11}$$

The substitutions according to Eq. 8 were used leading to discrete approximation

$$\mathbf{m}(z)=\frac{z^{-1}T_s\mathbf{K}_i}{1-z^{-1}}\mathbf{q}_{ref}(z)-\frac{\left(T_s\mathbf{K}_p+\mathbf{K}_d\right)+z^{-1}\left(\mathbf{K}_iT_s^2-T_s\mathbf{K}_p-2\mathbf{K}_d\right)+\mathbf{K}_dz^{-2}}{T_s-T_sz^{-1}}\mathbf{q}(z). \tag{12}$$

It was proved by simulation that this discrete form of the law obtained by such a way realizes a stable control of hexapod for sampling period, $T_s \geq 1\,ms$. Discrete representation of higher layer control law is analogical to representation in Fig. 3.

3.3. Referential time courses

Combination of top plate adjustment to operating position with consequent harmonic lagging of the plate which represents typical operation mode of device was used as referential time course of top plate movement (ie position and orientation of masspoint), see Fig. 4.

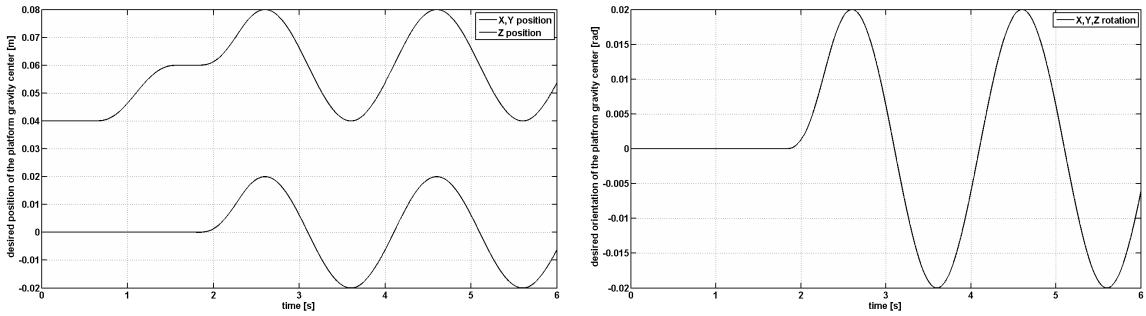

Fig. 4: Course of referential position a orientation (splined, see below)

Note that by the analysis of corresponding courses of motor driving voltages and shaft moments it was determined that the steps in acceleration of continuous referential signal cause impulses in motors driving voltage and extensive impulses in motors shaft moments (up to 300 % of maximum allowable value). The 5th order splines with smooth connection were used for elimination of this effect by bypassing the critical intervals in courses of referential trajectories. The comparison of both courses of driving voltage and shaft moment is shown in Fig. 5. Splined signal is delayed there by 1.2 s against undelayed.

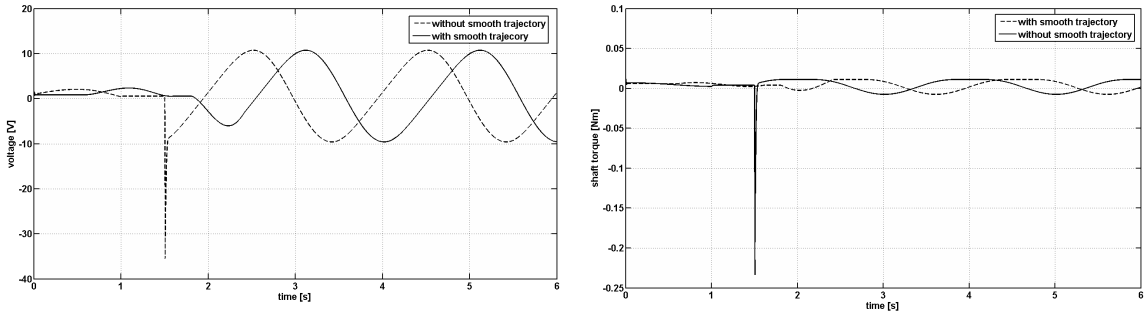

Fig. 5: Comparison of driving voltages and shaft moments

4. Reached results

Reached results demonstrate that the hexapod is controllable by relatively simple two–layer controller. Inaccuracy of top plate masspoint positioning is, for typical working mode of device, up to 4.2 % of masspoint movement rate (see Fig. 6). With respect to large variation of tested specimens parameters values (it is a case of spinal segments), this accuracy seems to be sufficient.

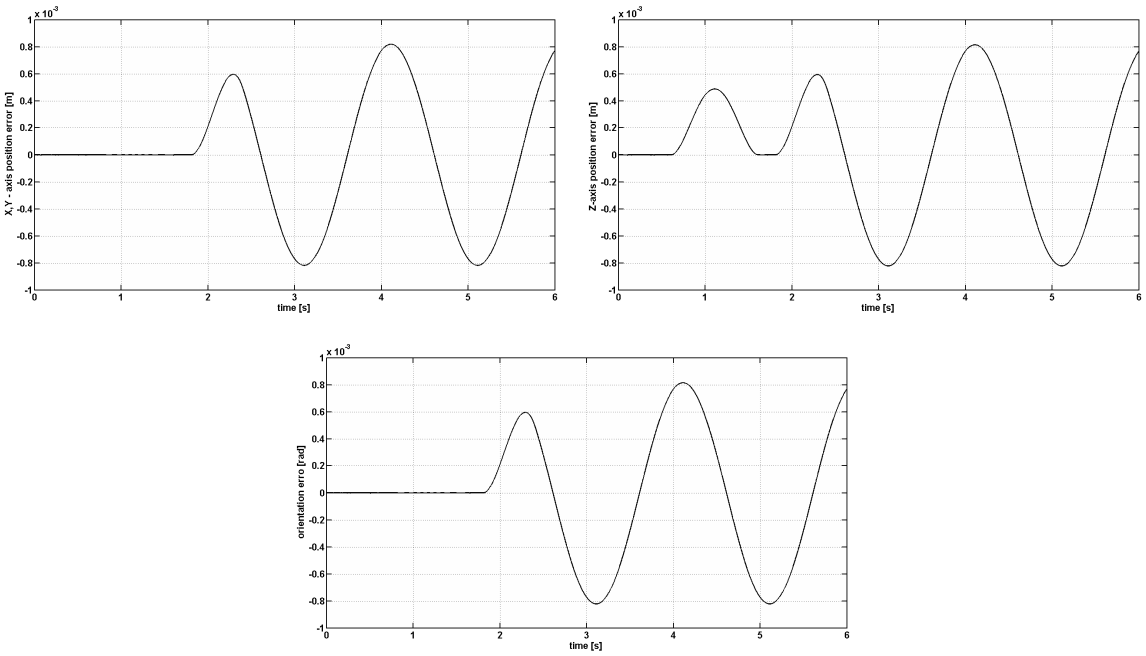

Fig. 6: Positioning errors in position (xy, z) a orientation

The accuracy decrease with increased configuration deviation of mechanism from working configuration can be explained by used methodology of control design: linear structure of control was designed with application of linearized hexapod model in neighborhood of working configuration. Higher accuracy could be reached, at the expense of more complicated control, by addition of nonlinear compensation elements.

With respect to small desired velocities of top plate positioning the elements compensated only kinematics of whole device should be sufficient.

5. Conclusions

Presented control is ready for implementation via discrete state controllers. The controllers have relatively simple structure (the higher control layer works with 12 states, the lower control layer with 6×2 states) and allow to tune eigenvalues of the hexapod. Satisfactory robustness of the proposed control was verified by numerous simulations.

Acknowledgement

Published results were acquired using the subsidization of the Ministry of Education, Youth and Sports of the Czech Republic, research plan MSM 0021630518 and the project 1P05ME789.

References

Merlet, J. P. (2005) Parallel robots, 2nd Edition. Kluwer, Dordrecht.

Passino, K. M. (2005) Biomimicry for Optimization, Control, and Automation. Springer, London.